# This article is published in:

# Dating Saharan dust deposits on Lanzarote (Canary Islands) by luminescence dating techniques and their implication for palaeoclimate reconstruction of NW Africa

*H. von Suchodoletz\*, M. Fuchs, and L. Zöller*

Department of Geomorphology, University of Bayreuth, Universitätsstrasse 30, D-95440 Bayreuth, Germany
(*hans.vonsuchodoletz@uni-bayreuth.de*)

Lava flow dammed valleys (Vegas) on Lanzarote (Canary Islands) represent unique sediment traps, filled with autochthonous volcanic material and allochthonous Saharan dust. These sediments and the intercalated palaeosoil sediments document past environmental change of the last glacial-interglacial cycles, both on Lanzarote and in NW Africa. A reliable chronology must be established to use these sediment archives for palaeoclimate reconstructions. Owing to the lack of organic material and the limiting time range of the ^{14}C-dating method, luminescence dating is the most promising method for these sediments. However, the fluvio-eolian character of these sediments is a major problem for luminescence dating, because these sediments are prone to insufficient resetting of the parent luminescence signal (bleaching) prior to sedimentation. To check for the best age estimates, we compare the bleaching behavior of (1) different grain sizes (coarse- versus fine-grain quartz OSL) and (2) different minerals (fine-grain feldspar IRSL versus fine-grain quartz OSL). The results show that owing to its bleaching characteristics, quartz is the preferable mineral for luminescence dating. On the basis of the fine- and coarse-grain quartz OSL age estimates, a chronostratigraphy up to 100 ka could be established. Beyond this age limit for OSL quartz, the chronostratigraphy could be extended up to 180 ka by correlating the vega sediments with dated marine sediment archives.

*Keywords:* luminescence dating; Saharan dust; Canary Islands; insufficient bleaching; land/sea correlation; human occupation.

## 1. Introduction
Lava flow dammed valleys (Vegas) on Lanzarote (Canary Islands) represent sediment traps, filled with autochthonous volcanic material and allochthonous Saharan dust. These sediments are regarded as unique terrestrial archives for the Quaternary paleoclimate reconstruction of northwest Africa (H. von Suchodoletz et al., Geomorphological investigations of sediment traps on Lanzarote (Canary Islands) as a key for the interpretation of a palaeoclimate archive off NWAfrica, submitted to Quaternary International, 2008) (hereinafter referred to as von Suchodoletz et al., submitted manuscript, 2008a).

There have been many attempts to reconstruct the paleoclimate for this region. Marine records that may extend back to the Tertiary [e.g., Dupont, 1993; Brunner and Maniscalco, 1998; Moreno et al., 2001] have the advantage that they provide continuous records with generally well-preserved proxies. In contrast, terrestrial archives are commonly discontinuous and represent only short periods, which makes their paleoclimate interpretation difficult [e.g., Gasse et al., 1987; Cheddadi et al., 1998; Lancaster et al., 2002]. However, despite the limitation of interpretation and hiatuses, terrestrial archives are essential for investigating paleoclimate on land, especially the regional patterns and the land-sea interaction. On the Eastern Canary Islands, various terrestrial archives have been used to reconstruct paleoclimate, for example, dune sequences and their intercalated paleosols [e.g., Rognon et al., 1989; Criado et al., 2004; Ortiz et al., 2006], calcretes [e.g., Alonso-Zarza and Silva, 2002], cave sediments [e.g., Coello et al., 1999] and marine terraces [e.g., Meco et al., 2002]. However, these archives show hiatuses and represent limited periods of the Quaternary. Our studies from Lanzarote, where thick Saharan dust had accumulated in volcanic valleys, reveal a generally continuous record, reaching from the Holocene to the Middle Pleistocene (Zöller

et al. [2003] and present study), which makes these sediments an outstanding terrestrial archive for a paleoenvironmental reconstruction of Lanzarote and NW Africa.

For paleoclimatic interpretation of these archives a sound chronostratigraphy is of crucial importance. Previous studies on the Eastern Canary Islands used the 14C-dating method [e.g., Petit-Maire et al., 1986] as well as U-Th ages [e.g., Hillaire-Marcel et al., 1995], but the results of both methods suffer from the fact that the ages were determined on land snail shells which may represent open systems. Therefore these dates must be regarded as provisional [Edwards and Meco, 2000]. The second shortfall of both methods is that they do not directly date the sedimentation process, a drawback that does not apply to luminescence dating. Sporadic studies from the Eastern Canary Islands using luminescence dating were presented by Pomel et al. [1985] and Bouab and Lamothe [1997]. Since our initial dating results using infrared stimulated luminescence (IRSL) were promising [Zöller et al., 2003], and in most parts of the investigated profiles there are neither organic matter nor land snail shells, we continued to built up our chronostratigraphy using luminescence dating. Luminescence dating is based on the fact that quartz and feldspar grains accumulate energy in their crystal lattice after burial, that increases in response to ionizing radiation to which the grains are exposed. This signal is discharged when the grains are exposed to sunlight. Measurement of this signal results in the equivalent dose (De). To determine the time that elapsed since the last bleaching, the De is divided by the ionizing radiation (dose rate, $\overset{.}{D}$ ) of the dated sediment [Singhvi and Krbetschek, 1996; Aitken, 1998; Wintle, 1998].

The advantage of luminescence dating is that it directly dates the last exposure to sunlight, but good optical bleaching prior to burial is of major importance. Pure eolian sediments such as loess show very good bleaching prior to sedimentation, and have been dated successfully for many years [e.g., Berger et al., 1992; Rousseau et al., 1998; Zöller et al., 2004]. It is only recently that the development of coarse-grain dating techniques using optically stimulated luminescence (OSL) facilitated the dating of poorly bleached materials, for example, fluvial, colluvial or playa sediments [e.g., Olley et al., 1998; Fuchs and Wagner, 2003; Bubenzer and Hilgers, 2003]. Being aware of the largely colluvial character of our sequences (von Suchodoletz et al., submitted manuscript, 2008), we have compared three different luminescence dating techniques (IRSL of fine-grained feldspars and OSL of fine and coarse-grained quartz) with different bleaching properties to build up a reliable chronostratigraphy for our archives. This methodological comparison should help to evaluate the reliability of the ''problematic'' IRSL dates in the older parts of the profiles, where they are the only numerical dating method available.


## 2. Study Area

Lanzarote (28°50'N-29°13'N, 13°25'W-13°52'W) belongs to the Canary Islands/Spain and is situated ∼130 km west of the southern Moroccan coast (Figure 1). It is a volcanic island, composed of basic to ultrabasic volcanic rocks. Volcanism started around 15.5 Ma ago and has persisted to recent historical times [e.g., Carracedo et al., 1998].

Owing to its limited altitude (maximum 670 m amsl), Lanzarote does not receive precipitation from rising trade winds. It receives 100 mm (at lower elevation) to 250 mm (at higher elevation) precipitation from boreal winter cyclones. Mean annual temperature is 19.9°C [Jahn, 1988]. Lanzarote is characterized by a very sparse, shrubby and disperse vegetation dominated by xerophytic and halophytic species manifesting a semi desert character.

The island is situated at the northern fringe of the Saharan dust plume over the North Atlantic Ocean. Dust is brought to the island during two different synoptic situations: During the first situation, dust is entrained by so called ''Calima'' winds: low-level continental African Trade winds (Harmattan) deflected toward the west by Atlantic cyclones especially during boreal winter [Criado and Dorta, 2003]. The second situation occurs exclusively during boreal

summer, when dust is advected by the northern branch of the high-altitude Saharan Air Layer. Subsequently, the material sinks into the lower atmosphere north of the Canary Islands and is finally transported toward the islands via the Northeast Trade wind [Koopmann, 1981; Bozzano et al., 2002]. Dust can be deposited here during both dry and wet conditions [Criado and Dorta, 2003; Menéndez et al., 2007].

## 3. Studied Sites

On Lanzarote, paleo-valleys of Miocence to Pliocene age were dammed during the Early and Middle Pleistocene by lava flows and pyroclastic material. Locally these valleys are called vegas. In our studies we used the outcrops situated in loam pits excavated during the past decades in the vegas of Feme´s, Guatiza and Teguise (Valle de San José) (Figure 1). All studied profiles were chosen in a distal position from geomorphologically active slopes. Hence we chose profile Guatiza III instead of Guatiza I and II [Zöller et al., 2003] for further investigations. Two vegas (Guatiza and Teguise) are situated on the fringes of the Famara Massif in the north of the island at a distance of ~6 km from each other. Damming of these valleys was never total, so hiatae can be expected. The valley of Femeés is located in the Los Ajaches Massif in the south of Lanzarote about 30 km from the northern sites, and damming was complete until today [Zöller et al., 2006].

The stratigraphies can be seen in Figure 2. The sediments are composed of interbedded in situ and reworked colluvial material originating from allochthonous Saharan dust and autochthonous volcanic products. Parts of these sediments were subject to pedogenesis and are consequently characterized by reddish color and a vertisol texture, whereas other layers are only slightly weathered and show a yellowish color and a silty granulometry. Some beds were overprinted by carbonatic waters and thus contain carbonate nodules, calcified root channels, or are fully developed as calcrete horizons. Many layers were overprinted by water containing Fe and Mn. Consequently, Fe and Mn stains and concretions occur, the largest in the vega of Teguise. In some horizons, calcified nests of anthophora bees are common. Whereas no coarse colluvial material is found in the lower parts of the sequences, the upper parts consist of anthropogenic colluvium containing pebbles and partly ovicaprid bones. In Femés, coarse volcanic fallout is observed between ~220 and 400 cm. The stratigraphy of this profile is slightly revised compared to that published by Zöller et al. [2003]. Consequently, in the case of differing depths both are indicated in Table 4 in section 4.3 and Table 5 in section 5.2. The properties of the sequences are listed in Table 1.

These sedimentary units record the landscape and paleoclimatic history from the Lower Pleistocene to the Holocene. The geomorphic system and its sedimentation processes are described in detail by von Suchodoletz et al. (submitted manuscript, 2008a).

## 4. Methods

For luminescence dating sampling took place during the night, after removing the outer 30 cm of the profile to avoid any contamination with lightexposed material. Sampling and sample preparation at the Bayreuth luminescence laboratory (University of Bayreuth/Germany) was done under subdued red light (wavelength $640 \pm 20$ nm).

### 4.1. Sample Preparation
#### 4.1.1. Coarse-Grain Quartz Samples
After sieving, the fraction 63-200 mm was treated with HCl and $H_2O_2$ to destroy carbonate and organic matter, and was held in an ultrasonic bath for 30 min to destroy aggregates. Heavy minerals (density > 2.75 g/cm3) and feldspars (density < 2.62 g/cm3) were separated in a lithium heteropolytungstate solution (LST). The quartz material was subsequently etched in 40% HF for 45 min in order to remove any remaining feldspar as well as the alpha irradiated outer layer of the quartz grains. The resultant material was fixed on aluminum cups

(diameter 12 mm) using silicone oil. The number of grains per cup was between 200 and 600, representing small aliquots according to Fuchs and Wagner [2003].

### 4.1.2. Fine-Grain Quartz Samples
To remove carbonates and organic carbon, the fraction <63 mm was treated with HCl and $H_2O_2$. Subsequent addition of 0.05 M sodium pyrophosphate and treatment in an ultrasonic bath for 30 min dispersed clays and destroyed grain aggregates. Extraction of the 4–11 mm fraction was done in Atterberg-settling tubes up to 50 times. The separated polymineral fraction 4–11 mm was etched for 4-5 days in pretreated 34% hexafluorosilicic acid to remove any remaining feldspars (for methodology, see Fuchs et al. [2005]). After a short IRSL test on two aliquots that included radiation (50 Gy) and IRSL measurement to identify any possible remaining feldspar contamination, the material was pipetted on to 9.6-mm aluminum discs.

### 4.1.3. Fine-Grain Polymineral Samples
The polymineral fine silt fraction was extracted as described above for fine-grain quartz samples and was directly pipetted on to aluminum discs (diameter 9.6 mm). Each disc had about 1.6 mg of silt.

## 4.2. Measurements
For measurements we used two Risø-Readers TL/OSL-DA-15 combined with a Thorn-EMI 9235QA photomultiplier [Bøtter-Jensen et al., 1999]. Sources used for radiation are listed in Table 2. The software Analyst 3.07b was used for analysis of the data.

### 4.2.1. Fine- and Coarse-Grain Quartz OSL
Measurement parameters of fine- and coarsegrain quartz samples are listed in Table 3. Equivalent doses (De) were determined using the single aliquot regenerative dose protocol (SAR) [see Murray and Wintle, 2000]. A saturating exponential growth curve was constructed, using six regeneration cycles after one measurement of the natural OSL: four measurements of regenerated doses, one repeated measurement of the first regenerated dose to determine the recycling ratio and one 0-dose regeneration cycle. The De was determined by subtracting the background from the used OSL integral. A check for possible feldspar contamination was done by stimulating the artificially irradiated samples with infrared and detecting in the blue range (390-450 nm). Depending on the availability of the prepared mineral fraction, we tried to measure a minimum of 30 aliquots from the coarsegrained fraction, and 6–7 aliquots from the finegrained samples. In individual cases, the number of measured aliquots was below 30 for coarse-grained samples. To determine a-values of the fine-grain samples, a-irradiation was used.

### 4.2.2. Polymineral IRSL
Measurement parameters for polymineral IRSL samples are listed in Table 3.
For De determination, the multiple aliquot additive dose protocol (MAAD) following Lang et al. [1996] was routinely used. After measurement of three natural and three artificially irradiated discs (test dose of 50 Gy) to obtain a rough approximation of the equivalent dose, six dose groups with five discs each were irradiated and stored for 1 month at room temperature. Subsequently, they were measured together with nine natural discs to construct the additive growth curve. The a-value of some representative samples was determined using an a-growth curve with three dose groups of three aliquots each.
Owing to limited laboratory capacity, we did not conduct tests for anomalous fading after Auclair et al. [2003], but used instead a simpler protocol following Lang et al. [1996]. We irradiated five discs with the highest irradiation dose, stored them for 3 months at room

temperature before measurement and compared them to the measurements done after 1 month of storage.

### *4.3. Dose Rate Determination*

The dose rate ($\dot{D}$) is the energy that accumulates in a mineral and thus creates the luminescence signal. The dose rate is composed of the natural radioactivity (α-, β-, γ-radiation) and the cosmic radiation affecting the sample. Since the outer rim of coarse grains are etched away using HF, α-radiation influences only the fine-grain material. Thus, for fine grains, the a-value giving the effectivity of α- compared to β-radiation must be determined.
We determined natural radioactivity by measuring the concentration of the radioactive elements U, Th and K using dry, ground material. U and Th contents were calculated using thick source α-counting (42 mm) at the University of Bayreuth. Potassium concentrations were measured at the Bayreuth Center for Ecology and Environmental Research (BayCEER), Bayreuth/Germany using inductively coupled plasma source mass spectrometry (ICPMS), and at the University of Marburg/Germany using an atomic adsorption spectrometer (AAS). Dose rates were calculated using the conversion factors given by Adamiec and Aitken [1998]. Cosmic dose rates were evaluated according to Prescott and Hutton [1994]. All dose rates are listed in Table 4.

### *4.4. Water Content*

For every sample the water content was measured gravimetrically. Since the outcrops have been open for many years and the sediments have been desiccated, measured values are obviously underestimations compared to the paleovalues as already stated by Zöller et al. [2003]. Thus, using the grain size distribution of a sample and the resulting middle pore volume, we estimated potential minimal and maximal water contents of a sample as described by Fuchs [2001]. For age calculation, an average value was taken. The error is assumed to be generally 0.1. Measured and corrected water contents are given in Table 4.

### *4.5. Age Calculation*

von Suchodoletz et al. (submitted manuscript, 2008a) demonstrate that most of the sediments filling the vegas are reworked and deposited by colluvial and fluvial processes. These processes are problematic for luminescence dating because they are occurring rather rapidly and often the finer material is transported in the form of aggregates. Hence bleaching of these sediments during colluvial transport was presumably not always complete, thus resulting in overestimated De values as detected in other studies [e.g., Porat et al., 2001; Fuchs and Wagner, 2003].
For fine grains, insufficient bleaching is not easily detectable since every disc contains thousands of grains giving a luminescence signal so that De differences between the discs are averaged. Instead, for coarse grains single aliquot and single grain methods offer the possibility to detect and correct insufficient bleaching by looking at their De scatter and the type of De distribution (Gaussian, left-skewed, right-skewed) [e.g., Olley et al., 1998; Lepper et al., 2000; Bailey and Arnold, 2006; Fuchs and Wagner, 2003]. Since most of our De distributions are positively skewed which may indicate insufficient bleaching, we had to find a way to obtain the De corresponding to the last reworking of the sediments. Different techniques were developed on the basis of the assumption that the last bleaching event is equivalent to the left maximum of a right skewed De distribution. However, some of these techniques are not applicable to our De distributions for different reasons: the approach of Olley et al. [1998] taking the lowest 5% of the De distribution is not applicable owing to a relatively broad rising limb of the De distribution resulting in greatly underestimated De. Accordingly, this method is generally judged to be useful only in case of young, poorly bleached fluvial samples [Bailey and Arnold, 2006]. The leading edge method developed by

Lepper et al. [2000] was inapplicable since the quantity of measured aliquots was not sufficient to get a good Gaussian fit through the rising limb of our distributions [cf. Fuchs et al., 2007]. The method of Fuchs and Lang [2001], using an empirically derived threshold to identify the well bleached proportion of an insufficiently bleached sample is also not applicable in our case. This is due to the fact that for many samples the threshold was already exceeded using the first two De from the sorted low to high De value data set. Thus we decided to use the approach of Juyal et al. [2006], modified by Fuchs et al. [2007]. Basically, this is a simplified minimum age model of Galbraith et al. [1999].

$$De = De_{min} + 2 * \sigma_{max} + 4\%$$

where $De_{min}$ is the minimal equivalent dose after subtraction of the lower 5% quantil (see below), $\sigma_{max}$ is the maximal error occurring in the data from the lower end to the first maximum of the De histogram and 4% are added as general instrumentation error of the used Risø reader.

A common problem is the mixing of younger material dropped through pedogenic cracks or root channels as described by Bateman et al. [2003]. We have observed this process in the vega of Guatiza. This phenomenon would cause an underestimation of the De and is visible as individual outliers not linked to the form of the De distribution toward lower values in many histograms (Figure 3). To neutralize this frequently occurring effect, we decided to subtract the lower 5%quantil of the sorted De distribution from all samples prior to statistical ccalculations. Depending on the number of measured aliquots, one to two De had to be rejected.

For fine grains, insufficient bleaching is hardly detectable. Thus the arithmetic mean of obtained De from the measurements was taken for age calculation. IRSL ages by Zöller et al. [2003] were recalculated using corrected water contents (see above) and new cosmic dose rates.

## 5. Results
## 5.1. Dose Rates

Results of dose rate ($\dot{D}$) determination are given in Table 4 with their 1s errors.

Uranium contents calculated from thicksource α-counting range from 1.46 to 3.1 ppm and thorium values from 5.0 to 10.7 ppm. Potassium contents determined either by AAS or ICPMS range from 1.7 to 4.1%. Rather low dose rate values generally occur in calcareous horizons (e.g., BT 318, BT 319, BT 308). The occurrence of radioactive disequilibria in calcareous horizons cannot be excluded. However, the U content of calcite presents only a very small proportion compared to the total Ucontent, so that desequilibria in the U-decay chain are not expected to have a significant influence on the total dose rate. Furthermore, Schäfer and Zöller [1996] demonstrated from a Middle Palaeolithic site in Thuringia/Germany showing significant disequilibria detected by lowlevel γ-spectrometry, that using dose rates from U and Th based on α-counting is a good approach if radioactive disequilibrium has regenerated more or less permanently since deposition. Carbonate precipitation posterior to deposition may dilute concentrations of radioelements and thus lower the dose rate. However, carbonate-free layers deposited over carbonate-rich beds indicate that secondary calcification was more or less contemporaneous to sedimentation. The consequences of this effect should not have played a major role although a slight underestimation of dose rates due to this effect cannot be excluded.

## 5.2. Equivalent Doses

Equivalent doses of quartz OSL and feldspar IRSL measurements are listed in Table 5 with their 1σ errors. Owing to their own characteristics and accuracies, the applied luminescence methods (coarse- and fine-grain OSL, fine-grain IRSL) are discussed separately.

### 5.2.1. Quartz Coarse-Grain OSL measurements

The potential for total bleaching of the investigated sediments was tested by exposure of the prepared coarse-grain quartz extracts to 10 hours of natural daylight (Bayreuth/Germany, ~50°N, November 2005) with a subsequent OSL measurement. This test was carried out for samples BT 190, BT 195 and BT 196 which showed no OSL signal after daylight exposure. Furthermore, a dose recovery test was carried out using the same samples as for the bleaching test. After the bleaching of the samples they were given b-radiations of 4.28 Gy (sample BT 195), 17.13 Gy (sample BT 196) and 38.55 Gy (sample BT 190). Subsequently, the OSL measurements for De determination were performed with preheat temperatures of 220°, 240°, 260° and 280°C, with four aliquots for each temperature. In Figure 4 the results of these measurements can be seen, with a De plateau between 220° and 280°C within error bars. Thus, in spite of a slight overestimation of given doses, for all further De measurements a preheat temperature of 240°C was applied.

All quartz samples show typical exponential saturating growth. From the growth curves it can be seen that saturation, on average, is reached around 350 Gy but can also be somewhat higher for several samples. Thus highest De estimations above 300 Gy have to be treated with caution.

Measured aliquots were excluded from further analysis when test dose error, paleodose error, or recycling ratio error were >10%. The same applies to aliquots giving a signal less than three times the standard deviation of the background. This was true for about 7% of the measured aliquots.

### 5.2.2. Quartz fine-grain OSL measurements

Fine-grain OSL De range from 5.6 to 211 Gy. The frequency distribution of the measured aliquots per sample yielded a standard deviation between 2 to 12%. About 3% of the measured aliquots had to be removed owing to the exclusion criteria defined above. All growth curves show an exponential behavior, with saturation attained around 350 Gy (highest calculated De = 211 Gy). Typical measurements of a-values range between 0.03 and 0.05. Consequently, a mean value of 0.04 was used for calculations.

### 5.2.3. IRSL fine-grain measurements

As can be seen from the IRSL growth curves, saturation of the investigated feldspars is attained around 1800-2000 Gy. Hence all investigated samples (highest De ~700 Gy) are within the datable dose range. IRSL growth curves from Lower to Middle Holocene samples show an almost linear behavior, whereas the older ones are clearly saturating exponential. Fitting error of the growth curves was between 0.3 and 3.5%, giving lower values for higher doses. As already stated by Pomel et al. [1985], measured a-values are very low with values between 0.029 and 0.063, being in general higher in Teguise (average 0.06) than in Femés (average 0.04) and Guatiza (average 0.05). Owing to long a-irradiation times only some representative a-values were determined, whereas for the missing values the mean for every profile was taken. Almost half of the samples show significant anomalous fading up to 40%.

## 6. Discussion
### 6.1. Reliability of different luminescence methods
### 6.1.1. Coarse-Grain OSL Ages
Most of our coarse-grain single aliquot histograms are right skewed (mean skewness 1.24),

indicating insufficient bleaching during colluvial transport. Several outliers toward lower doses were also observed (Figure 3).

Owing to the strong scatter of the equivalent doses, age errors are between 9 and 31%. The occurrence of colluvial reworking during most periods was also proven by micromorphological studies [Sauer and Zöller, 2006]. This occurs in all vegas, however the histogram asymmetry is generally lower in Teguise compared to Femés and Guatiza III. This is explained by the lower catchment area-valley bottom ratio, which means a lower proportion of (insufficiently bleached) colluvial material originating from the slopes relative to in situ eolian dust is found in the vega bottom sediments (von Suchodoletz et al., submitted manuscript, 2008). Correspondingly, lowest errors were observed in the vega of Teguise. Using the approach of Juyal et al. [2006], most De values are now situated at the upper rising left limb of our distribution (Figure 3). Here we believe that the equivalent doses corresponding to the last bleaching event should be located. The general omission of the lower 5% of measured aliquots from all samples strongly improved our De calculation in samples exhibiting outliers toward the lower end of the distribution, and thus De of most of these samples fall at the upper rising limb of our histograms as well. In cases without outliers, owing to the broad rising limb, the resulting shift toward higher De is very small. Thus this method appears to be a justified approach for De determination.

For two samples, however, this approach seems to fail: Sample BT 200 shows an exceptional De histogram with a left skewed distribution (Figure 5a). Since the De of this sample is close to saturation level it is very likely that the aliquots normally forming the right (older) tail of the distribution were already in saturation and thus are not present in the histogram. Additionally, the number of aliquots is strongly limited so that a rising limb is not well developed. The arithmetic mean De of this sample gives a value at the rising limb close to the first maximum of the distribution (Figure 5a). However, owing to the non-Gaussian form of the distribution this arithmetic mean can only be a rough estimation. Caused by the limited amount of aliquots, the calculated De of sample BT 197 may be underestimated and should be regarded as a minimum age (Figure 5b).

Luminescence tests investigating insufficient bleaching (due to iron stains around the grains) during aeolian transport were carried out with recent Saharan dust from the Canary Islands (H. von Suchodoletz et al., Luminescence bleaching characteristics of Saharan dust – A case study from Lanzarote, Canary Islands (Spain), submitted to Quaternary Geochronology, 2008) (hereinafter referred to as von Suchodoletz et al., submitted manuscript, 2008b). They show that for coarse grains inherited doses with respect to dose rates from Lanzarote are in the range of only 0.1-0.2 ka and are thus negligible. A sample from colluvial material overlying a historic lava flow dating from 1736 AD (sample BT 204) yields an apparent coarse-grain OSL age of about 1.2 ka, thus indicating an overestimation <1 ka. These tests show that coarse-grain OSL basically offers the required conditions for dating Lower Holocene or older fluvio-eolian sediments. The problem of a slight overestimation of given doses during the preheat tests (see Figure 4) must be seen against the background of generally relatively large errors of coarse-grain OSL ages:owing to the uncertainty caused by insufficient bleaching, dating errors are rather large, so that the overestimation effect is smaller than calculated errors. This shows, however, that our luminescence ages are points of reference rather than precise dates.

### 6.1.2. Fine-Grain Quartz OSL Ages

Comparison of coarse and fine-grain quartz OSL ages reveals that the latter do not show significant age overestimations as could be expected owing to insufficient bleaching. Young Holocene samples show, however, a regular overestimation of about 1 to 3 ka. (samples BT 189, BT 198, BT 310). Overestimation of the same magnitude is found for recent sample BT 204. Thus bleaching of fine grains is not as complete as for coarse-grain OSL. This could be due to their colluvial transport as aggregates. Since quartz OSL does not exhibit anomalous

fading [Aitken, 1998], fine-grain quartz OSL yielded reasonable ages in a suitable time interval. Additionally, it provides consistent ages for parts of the sedimentary sequence where owing to the lack of fine sand or the occurrence of anomalous fading, neither coarse-grain OSL nor reliable IRSL ages are available. This was the case for samples BT 304 and BT 305.

### 6.1.3. Fine-Grain IRSL Ages

Depending on the dose rate, the OSL of quartz from Lanzarote saturates between 100 and 130 ka. Thus, owing to their higher saturation level, only IRSL feldspar ages are available in the lower parts of the profiles. Anomalous fading that was detected during the fading tests for almost half of the samples (see Table 5) is a problem. This could be due to the properties of local volcanic plagioclases as described by Wintle [1973], although no correlation between the fading rate and volcanic input could be found.

Even if anomalous fading was not detected during the test, the so called midterm fading cannot be excluded [Xie and Aitken, 1991]. For instance, the age of sample BT 304 is underestimated compared to the fine-grain OSL age, even though the former exhibits no anomalous fading during the test. In this case midterm fading can possibly be the cause. Another possible cause for age uncertainty is insufficient bleaching: since colluvial transport of fine grains takes mostly place as aggregates, they are more vulnerable to insufficient bleaching than coarse grains as shown for fine-grain OSL ages above. A third possibility could be the somewhat slower bleaching of feldspar IRSL compared to quartz OSL [Godfrey-Smith et al., 1988]. Furthermore, an effect described by Trautmann et al. [2000] could cause unreliable ages: above ~800 Gy the IRSL-signal of potassium feldspars may be expected not to grow in a single exponential manner during artificial irradiation. Above this threshold, radiofluorescence of K-feldspars already slows down more than expected, indicating the failure of further conduction band-electron trap transition. A further growth of the IRSL signal beyond an absorbed dose of _800 Gy may thus not directly be connected to electron filling of traps carrying the correct age information. Thus extrapolations using these dose points are problematic. It should be noted, however, that so far Trautmann et al. [2000] stated this effect for K-feldspars only.

In order to check the reliability of IRSL ages suspected of potentially showing much larger age overestimations in comparison to coarse-grain OSL ages, we conducted double measurements of finegrain IRSL and coarse-grain OSL in the younger parts of the profiles. These show that, within error limits, 8 out of 16 double measurements yield IRSL ages in agreement with coarse-grain OSL. Two IRSL ages (samples BT 199 and BT 224) are overestimated by 20-25 ka compared to coarsegrain OSL ages. In case of sample BT 199, this strong overestimation occurs despite strong anomalous fading. Although samples BT 189 and BT 200 show signals close to real palaeodoses today, we assume that they originally had an inherited signal during burial since they show substantial anomalous fading that reduced the original signal. In case of sample BT 189 exhibiting similar IRSL De and fine-grain OSL De, an original higher IRSL De compared to the OSL De was eventually caused by the slower bleaching of feldspar compared to quartz [Godfrey-Smith et al., 1988]. In total, insufficient bleaching obviously affects almost 30% of the IRSL test samples. Therefore IRSL ages from the lower parts of the profiles that are not corroborated by coarse-grain OSL ages should be considered with caution.

Looking at young Holocene samples, Looking at young Holocene samples, finegrain IRSL ages are regularly overestimated by 0.5 to 3 ka (samples BT 193, BT 195, BT 198) compared to coarse-grain OSL ages. Overestimation of the same magnitude is found for a recent sample (BT 204) taken above a lava flow dating from 1736 AD, as well as for recently investigated present-day dust exhibiting a residual IRSL-dose equivalent to <0.93 ka. For fine-grain OSL ages, overestimation is in the same range as for IRSL ages. This indicates that at least a part of the overestimation is due to a residual dose that existed prior to the arrival of Saharan dust

at Lanzarote, possibly caused by aggregation during transport (von Suchodoletz et al., submitted manuscript, 2008b). This effect is negligible for older samples, but Middle Holocene IRSL ages like some of those published by Zöller et al. [2003] should be regarded with care: remeasurement of IRSL sample BN-D 219 from profile Guatiza I giving an IRSL age of 4.3 ± 0.5 ka yielded an age of 1.2 ± 0.1 ka using coarse-grain quartz OSL.

## 6.2. Establishing a Chronostratigraphy

Considering the uncertainties of the applied luminescence methods and the lack of independent dating methods, coarse-grain OSL dating yields the most reliable dates since it offers the only possibility to recognize insufficient bleaching. Thus we regard these ages as the age base of our chronostratigraphical model.

Owing to the uncertainty even when using that method, we have to look for a possibility to correlate proxies yielded from the vegas with those from other studies. The composition of eolian components of the vega fillings should be similar to that from nearby marine cores. However, owing to the intermixed in situ and colluvial material of the vegas, this can only be recognized at ka timescales (von Suchodoletz et al., submitted manuscript, 2008a).

Kaolinite, a mineral originating from the Southern Sahara/Sahel belt [Caquineau et al., 1998] was found in variable quantities in our archives using semiquantitative XRD measurements. Since eolian quartz and kaolinite contents exhibit, except for the upper profile in Teguise, an almost identical pattern (von Suchodoletz et al., Loess-like and palaeosol sediments from Lanzarote (Canary Islands/Spain)—Indicators of palaeoenvironmental change during the Late Quaternary, submitted to Palaeogeography, Palaeoclimatology, Palaeoecology, 2008), a formation or destruction of kaolinite can mostly be excluded here. A marine study from the Northern Canary Basin about 300 km north of Lanzarote investigated the wind system off NW Africa and interpreted the aluminum content in core GeoB 5559-2 as a tracer of kaolinite that was brought to the study area by southerly winds [Moreno et al., 2001]. Likewise, another nearby marine study [Bozzano et al., 2002] interpreted iron contents in core GeoB 4205-2 as derived from the Southern Sahara/Sahel belt (for core locations, see Figure 1). Both proxies show good agreement with each other (Figure 6). The marine stratigraphies use the stable oxygen isotopes of fine-fraction carbonate (GeoB 5559-2) and of the planktonic foraminifera Globigerinoides ruber (GeoB 4205-2) for correlation with the established marine oxygen isotope stratigraphy of Martinson et al. [1987]. Owing to assumed similar wind systems over Lanzarote and the North Canary Basin, our kaolinite contents should exhibit the same pattern as the marine proxies. We therefore correlated marine aluminum and iron concentrations with kaolinite contents of our vega sediments, using the chronology established by the coarsegrain OSL ages. From this correlation, a similarity is identifiable between the marine proxies and kaolinite contents from the upper parts of our profiles Feme's and Guatiza III, whereas this pattern is biased in Teguise (Figure 6). In the latter vega, we found large concretions and ubiquitous coatings of ferromanganese character. These indicate that the biased signal could be due to stronger pedogenic mixing and kaolinite destruction generated by higher humidity and a more intensive iron and manganese dynamics here compared to the other vegas [Hurst and Kunkle, 1985].

However, this drawback could be overcome by a cross correlation of sedimentary stratigraphies and luminescence ages from the different vegas, supported by the correlation with the marine proxies. The resulting coherent chronological pattern results in fundamental conclusions concerning the different luminescence methods (see Figure 7). (1) If the result from sample BT 197 is regarded as a minimum age, almost 80% (n = 29) of the coarse-grain quartz OSL ages appear to be conclusive within their error bars. (2) Taking into account the effects of strong anomalous fading but disregarding the overestimation of a few ka in very young samples, only about 50% (n = 14) of the fine-grain IRSL samples yield correct ages

within their error bars. (3) Disregarding the overestimation of a few ka in very young samples, >80% (n = 6) of the fine-grain quartz OSL ages are consistent within their error bars.

The high rate of concordant coarse and finegrain quartz OSL ages, coherent during the cross correlation demonstrates that the obvious correlation pattern of local kaolinite with marine proxies can be confirmed. Unfortunately, reliable luminescence dating of the older parts of the profiles is not possible owing to anomalous fading and insufficient bleaching of the IRSL signal.

Thus, beyond the range of quartz OSL dating (between about 100 to 130 ka), having no reliable luminescence dates we tried to continue the correlation between local kaolinite in Femés and the marine proxies in order to build up a tentative chronostratigraphy. However, this correlation must be regarded as tentative. Following this correlation, IRSL ages from Femés older than 100 ka (samples BT 191, BT 303, BN-D 213) would overestimate burial ages by around 20 to 30 ka (Figure 7), which in case of sample BN-D 213 would be close to its 1σ confidence interval. In turn, in Teguise the two lowermost IRSL ages (samples BT 201 and 202) would by far underestimate burial ages of sediments when extrapolating the cross correlation with the stratigraphy of Feme´s, and with marine proxies. This underestimation in Teguise is also visible in Figure 7, where the IRSL ages indicate a strongly enhanced sedimentation rate prior to 130 ka not seen in Femés and not probable in the extremely materiallimited vega system of Teguise (lowest vega bottom/catchment area ratio). Thus the agreement of the ages of the lowest samples in Femés (BN-D 213) and Teguise (BT 202) within error bars seems not to be an argument for similar ages of the concerned layers, and sample BT 202 must be regarded as strongly underestimated in spite of the lack of anomalous fading. This underestimated age could thus either be due to midterm fading [Xie and Aitken, 1991] or to the effect described by Trautmann et al. [2000] as mentioned above. In contrast, the underestimation of sample BT 201 is explainable by strong anomalous fading.

Our chronostratigraphy shows that in all vegas, above a ubiquitously found unweathered llayer, certainly anthropogenically triggered colluvia, often including ovicaprid bones occur, varying in thickness between 0.55 m in Feme´s and 4.2 m in Guatiza III [see Zöller et al., 2003; von Suchodoletz et al., submitted manuscript, 2008a] (Figure 2). The beginning of these colluvia is dated between ~2.5 and 5 ka and probably marks the beginning of human activity on the island. Thus human activity probably started later than 5–10 ka as proposed by Zöller et al. [2003], but also somewhat earlier than the first century AC as assumed by Criado and Atoche-Peña [2004].

During Upper MIS 3 and Lower MIS 2, a hiatus seems to be present in all vegas. Whereas it can clearly be detected in Feme´s and Guatiza between about 15 and 30 ka, owing to the lower time resolution it is difficult to detect in Teguise where it may exist between about 8.5 (sample BT 198) and 22 ka (sample BT 235). In Teguise, this hiatus would be located at the same stratigraphic position as a clearly visible one observed in another outcrop of the same vega, near the incomplete damming in the south. The hiatuses in the vegas of Teguise and Guatiza are explainable by erosion caused by the incomplete damming of the sediment traps. Rognon and Coudé-Gaussen [1987] describe a ''geomorphological crisis'' in Fuerteventura and NW Morocco from 14 to 11 ka BP (equivalent to about 12.8–17.4 cal ka BP using the program calpal-online). This crisis was characterized by strong erosion due to heavy precipitation. The temporal coincidence with the hiatae observed in the incompletely dammed vegas Guatiza and Teguise makes this crisis a probable cause. In Femés, however, the hiatus is hard to explain owing to the low position of the profile in the vega bottom and the completely closed sediment trap.

It emerges that the bottom of profile Guatiza III has the youngest age, starting only at the beginning of MIS 3. When taking the tentative chronostratigraphy of the lower parts of profiles Femés and Teguise based on correlations, the maximum age of the exposed sequence in the vega of Femés would be around 175-180 ka, thus reaching back to the beginning of

Marine Isotope Stage (MIS) 6. Owing to the low sedimentation rate caused by a low catchment area-vega bottom ratio (von Suchodoletz et al., submitted manuscript, 2008a), the profile of Teguise appears to reach back farthest into the past. Extrapolating the average sedimentation rate of the upper dated part to the bottom, a maximal sedimentation age of about 300–350 ka could be expected for this profile.

## 7. Conclusions

Luminescence dating faces some problems in the vegas of Lanzarote. This is due to the fluvioeolian geomorphic dynamics with its inherent insufficient bleaching of the sediments as well as to strong anomalous fading of the IRSL signals probably caused by volcanic plagioclases. However, these problems could be overcome by using a combination of OSL datings as well as stratigraphic cross correlations between different profiles supported by correlations with nearby marine proxies, giving credibility to the chronology of the profiles. Consequently, a sound chronostratigraphy based on luminescence datings could be established until around 130 ka, whereas for the period between 130 and 180 ka a tentative chronostratigraphy is based on correlations and thus needs to be further confirmed (Figure 6). Altogether, this age model can serve as a timescale for paleoclimatic interpretations derived from the vegas.

## References

- Adamiec, G., and M. Aitken (1998), Dose-rate conversion factors: Update, Ancient TL, 16, 37–50.
- Aitken, M. J. (1998), An Introduction to Optical Dating, Oxford Univ. Press, 267 pp., New York.
- Alonso-Zarza, A. M., and P. G. Silva (2002), Quaternary laminar calcretes with bee nests: Evidences of small-scale climatic fluctuations, Eastern Canary Islands, Spain, Palaeogeogr. Palaeoclimatol. Palaeoecol., 178, 119–135.
- Auclair, M., M. Lamothe, and S. Huot (2003), The measurement of anomalous fading for feldspar IRSL using SAR, Radiat. Meas., 37, 487–492.
- Bailey, R. M., and R. J. Arnold (2006), Statistical modelling of single grain quartz De distributions and an assessment of procedures for estimating burial dose, Quat. Sci. Rev., 25, 2475–2502.
- Bateman, M. D., C. D. Frederick, M. K. Jaiswal, and A. K. Singhvi (2003), investigations into the potential effects of pedoturbation on luminescence dating, Quat. Sci. Rev., 22, 1169–1176.
- Berger, G. W., B. J. Pillans, and A. S. Palmer (1992), Dating loess up to 800 ka by thermoluminescence, Geology, 20, 403–406.

- Bøtter-Jensen, L., G. A. T. Duller, A. S. Murray, and D. Banerjee (1999), Blue light emitting diodes for optical stimulation of quartz in retrospective dosimetry and dating, Radiat. Prot. Dosim., 84, 335–340.
- Bouab, N., and M. Lamothe (1997), Geochronological framework for the Quaternary paleoclimatic record of the Rosa Negra section (Fuerteventura-Canary Islands, Spain), in Climates of the Past: Proceedings of the International Union of Geological Sciences, edited by J. Meco and N. Petit-Maire, pp. 37–42, Univ. de Las Palmas de Gran Canaria, Las Palmas de Gran Canaria, Spain.
- Bozzano, G., H. Kuhlmann, and B. Alonso (2002), Storminess control over African dust input to the Moroccan Atlantic margin (NW Africa) at the time of maxima boreal summer insolation: A record of the last 220 kyr, Paleogeogr. Paleoclimatol. Paleoecol., 183, 155–168.
- Brunner, C. A., and R. Maniscalco (1998), Late Pliocene and Quaternary paleoceanography of the Canary Island Region inferred from planctonic foraminifer assemblages of site 953, Proc. Ocean Drill. Program Sci. Results, 157, 73–82.
- Bubenzer, O., and A. Hilgers (2003), Luminescence-dating of Holocene playa sediments of the Egyptian Plateau Western Desert, Quat. Sci. Rev., 22, 1077–1084.
- Caquineau, S., A. Gaudichet, L. Gomes, M.-C. Magonthier, and B. Chatenet (1998), Saharan dust: Clay ratio as a relevant tracer to assess the origin of soil-derived aerosols, Geophys. Res. Lett., 25(7), 983–986.
- Carracedo, J. C., S. Day, H. Guillou, E. Rodrı´guez-Badiola, J. A. Canas, and F. J. Pe´rez-Torrado (1998), Hotspot volcanism close to a passive continental margin: The Canary Islands, Geol. Mag., 135(5), 591–604.
- Cheddadi, R., H. F. Lamb, J. Guiot, and S. van der Kaars (1998), Holocene climate change in Morocco: A quantitative´reconstruction from pollen data, Clim. Dyn., 14, 883–890.
- Coello, J. J., C. Castillo, and E. M. Gonza´lez (1999), Stratigraphy, chronology, and paleoenvironmental reconstruction of the quaternary sedimentary infilling of a volcanic tube in Fuerteventura, Canary Islands, Quat. Res., 52, 360–368.
- Criado, C., and P. Atoche-Pen˜a (2004), Influyó la ganadería de los mahos en el deterioro paleoambiental de la isla de Lanzarote?, Tenique Rev. Cult. Pop. Canaria, 6, 137–157.
- Criado, C., and P. Dorta (2003), An unusual 'blood rain' over the Canary Islands (Spain): The storm of January 1999, J. Arid Environ., 55, 765–783.
- Criado, C., H. Guillou, A. Hansen, C. Hansen, P. Lillo, J. M. Torres, and A. Naranjo (2004), Geomorphological evolution of parque natural de Las Dunas de Corralejo (Fuerteventura. Canary Islands), in Contribuciones recientes sobre geomorfología. (Actas de la VIII Reunio´n de Geomorfologı´a, Toledo, 22–25 de septiembre de 2004), edited by G. Benito and A. Diez-Herrero, pp. 291 – 297, Cons. Super. de Invest. Cient., Madrid.
- Dupont, L. M. (1993), Vegetation zones in NW Africa during the Brunhes chron reconstructed from marine palynological data, Quat. Sci. Rev., 12, 189–202.
- Edwards, N., and J. Meco (2000), Morphology and paleoenvironment of brood cells of Quaternary ground-nesting solitary bees (Hymenoptera. Apidae) from Fuerteventura, Canary Islands, Spain, Proc. Geol. Assoc., 111, 173–183.
- Fuchs, M. (2001), Die OSL-Datierung von Archäosedimenten zur Rekonstruktion anthropogen bedingter Sedimentumlagerung, Ph.D. thesis, 179 pp., Univ. of Heidelberg, Heidelberg, Germany.
- Fuchs, M., and A. Lang (2001), OSL dating of coarse-grain fluvial quartz using single-aliquot protocols on sediments from NE Peloponnes, Greece, Quat. Sci. Rev., 20, 783–787.

- Fuchs, M., and G. A. Wagner (2003), Recognition of insufficient bleaching by small aliquots of quartz for reconstructing soil erosion in Greece, Quat. Sci. Rev., 22, 1161–1167.
- Fuchs, M., J. Straub, and L. Zöller (2005), Residual luminescence signals of recent river flood sediments: A comparison between quartz and feldspar of fine- and coarse-grain sediments, Ancient TL, 23, 25–30.
- Fuchs, M., C. Woda, and A. Bu̇rkert (2007), Chronostratigraphy of a sediment record from the Hajar mountain range in north Oman: Implications for optical dating of insufficiently bleached sediments, Quat. Geochronol., 2, 202–207.
- Galbraith, R. F., R. G. Roberts, G. M. Laslett, H. Yoshida, and J. M. Olley (1999), Optical dating of single and multiple grains of quartz from Jinmium Rock Shelter, Northern Australia: Part I: experimental design and statistical models, Archaeometry, 41, 339–364.
- Gasse, F., J. C. Fontes, J. C. Plaziat, P. Carbonel, I. Kaczmarska, P. de Deckker, I. Soulié-Marsche, Y. Callot, and P. A. Dupeuble (1987), Biological remains, geochemistry and stable isotopes for the reconstruction of environmental and hydrological changes in the Holocene lakes from North Sahara, Paleogeogr. Paleoclimatol. Paleoecol., 60, 1–46.
- Godfrey-Smith, D. I., D. J. Huntley, and W. H. Chen (1988), Optical dating studies of quartz and feldspar extracts, Quat. Sci. Rev., 7, 373–380.
- Hillaire-Marcel, C., B. Ghaleb, and C. Gariépy (1995), U-series dating by the TIMS technique of land snails from paleosols in the Canary Islands, Quat. Res., 44, 276–282.
- Hurst, V. J., and A. C. Kunkle (1985), Dehydroxylation, rehydroxylation, and stability of kaolinite, Clays Clay Miner., 33(1), 1–14.
- Instituto Tecnológico y Geominero de España (2008), Mapa geológico de España, Memoríade la hoja geológica de la Isla de Lanzarote, scale 1:100.000, Madrid, Spain, in press.
- Jahn, R. (1988), Böden Lanzarotes, Ph.D. thesis, 175 pp., Univ. of Stuttgart-Hohenheim, Stuttgart, Germany.
- Juyal, N., L. S. Chamyal, S. Bhandari, R. Bhushan, and A. K. Singhvi (2006), Continental record of the southwest monsoon during the last 130 ka: Evidence from the southern margin of the Thar desert, India, Quat. Sci. Rev., 25, 2632–2650.
- Koopmann, B. (1981), Sedimentation von Saharastaub im subtropischen Nordatlantik während der letzten 25 000 Jahre, Meteor Forschungsergeb., C/35, 23–59.
- Lancaster, N., G. Kocurek, A. Singhvi, V. Pandey, M. Deynoux, J. F. Ghienne, and K. Lo (2002), Late Pleistocene and Holocene dune activity and wind regimes in the western Sahara desert of Mauritania, Geology, 30(11), 991–994.
- Lang, A., S. Lindauer, R. Kuhn, and G. A. Wagner (1996), Procedures used for optically and infrared stimulated luminescence dating of sediments in Heidelberg, Ancient TL, 14, 7–11.
- Lepper, K., N. A. Larsen, and S. W. S. McKeever (2000), Equivalent dose distribution analysis of Holocene eolian and fluvial quartz sands from Central Oklahoma, Radiat. Meas., 32, 603–608.
- Martinson, D. G., N. G. Pisias, J. D. Hays, J. Imbrie, T. C. Moore, and N. J. Shackleton (1987), Age dating and the orbital theory of the Ice Ages: Development of a high-resolution 0 to 300,000-year chronostratigraphy, Quat. Res., 27, 1–29.
- Meco, J., H. Guillou, J.-C. Carracedo, A. Lomoschitz, A.-J. G. Ramos, and J.-J. Rodríguez-Yánez (2002), The maximum warmings of the Pleistocene world climate recorded in the Canary Islands, Paleogeogr. Paleoclimatol. Paleoecol., 185, 197–210.

- Menéndez, I., J. L. Diaz-Hernandez, J. Mangas, I. Alsonso, and P.-J. Sanchez-Soto (2007), Airborne dust accumulation and soil development in the North-East sector of Gran Canaria (Canary Islands, Spain), J. Arid Environ., 71, 57–81.
- Moreno, A., J. Taragona, J. Henderiks,M. Canals, T. Freudenthal, and H. Meggers (2001), Orbital forcing of dust supply to the North Canary Basin over the last 250 kyr, Quat. Sci. Rev., 20, 1327–1339.
- Murray, A., and A. Wintle (2000), Luminescence dating of quartz using an improved single-aliquot regenerative-dose protocol, Radiat. Meas., 32, 57–73.
- Olley, J., G. Caitcheon, and A. Murray (1998), The distribution of apparent dose as determined by optically stimulated luminescence in small aliquots of fluvial quartz: Implications for dating young sediments, Quat. Geochronol., 17, 1033–1040.
- Ortiz, J. E., T. Torres, Y. Yanes, C. Castillo, J. de la Nuez, M. Ibanez, and M. R. Alonso (2006), Climatic cycles inferred from the aminostratigraphy and aminochronology of Quaternary dunes and paleosols from the eastern islands of the Canary Archipelago, J. Quat. Sci., 21(3), 287–306.
- Petit-Maire, N., G. Delibrias, J. Meco, S. Pomel, and J.-C. Rosso (1986), Paléoclimatologie des Canaries orientales (Fuerteventura), C. R. Acad. Sci. Ser. II, 303(13), 1241–1246.
- Pomel, R.-S., D. Miallier, J. Fain, and S. Sanzelle (1985), Datation d'un sol brun-rouge calcife`re par une coulée volcanique d'âge Würm ancien (51.000 ans) à Fuerteventura (Iles Canaries), Mediterranée, 4, 59–68.
- Porat, N., E. Zilberman, R. Amit, and Y. Enzel (2001), Residual ages of modern sediments in an hyperarid region, Israel, Quat. Sci. Rev., 20, 795–798.
- Prescott, J. R., and J. T. Hutton (1994), Cosmic ray contributions to dose rates for luminescence and ESR dating: Large depths and long-term time variations, Radiat. Meas., 23, 497–500.
- Rognon, P., and G. Coudeé-Gaussen (1987), Changements dans les circulations atmosphérique et océanique à la latitude des Canaries et du Maroc entre les stades isotopiques 2 et 1, Quaternaire, 7(4), 197–206.
- Rognon, P., G. Coude´-Gaussen, M.-N. Le Coustumer, J. C. Balouet, and S. Occhietti (1989), Le massif dunaire de Jandía (Fuerteventura, Canaries): Évolution des paléoenvironnements de 20.000 BP a` l'actuel, Int. J. Fr. Quat. Assoc., 37, 31–37.
- Rousseau, D.-D., L. Zöller, and J.-P. Valet (1998), Late Pleistocene climatic variations at Achenheim, France, based on magnetic susceptibility and TL chronology of loess, Quat. Res., 49, 255–263.
- Sauer, D., and L. Zöller (2006), Mikromorphologie der Paläoböden der Profile Femés und Guatiza, Lanzarote, Bayreuther Geowiss. Arb., 27, 105–130.
- Schäfer, D., and L. Zöller (1996), Zur Charakterisierung des weichselzeitlichen Freilandfundplatzes vom Gamsenberg bei Oppurg/Thüringen, Tübinger Monogr. Urgeschichte, 11, 235–246.
- Singhvi, A. K., and M. R. Krbetschek (1996), Luminescence dating: A review and a perspective for arid zone sediments, Ann. Arid Zone, 35(3), 249–279.
- Trautmann, T., M. R. Krbetschek, A. Dietrich, and W. Stolz (2000), The basic principle of radioluminescence dating and a localized transition model, Radiat. Meas., 32, 487–492.
- Wintle, A. G. (1973), Anomalous fading of thermoluminescence in mineral samples, Nature, 245, 143–144.
- Wintle, A. G. (1998), Luminescence dating: Laboratory procedures and protocols, Radiat. Meas., 27, 769–817.
- Xie, J., and M. J. Aitken (1991), The hypothesis of mid-term fading and its trial on Chinese loess, Ancient TL, 9, 21–25.

- Zöller, L., H. von Suchodoletz, and N. Küster (2003), Geoarchaeological and chronometrical evidence of early human occupation on Lanzarote (Canary Islands), Quat. Sci. Rev., 22, 1299–1307.
- Zöller, L., D.-D. Rousseau, K.-D. Jäger, and G. Kukla (2004), Last interglacial, Lower and Middle Weichselian—A comparative study from the Upper Rhine and Thuringian loess areas, Z. Geomorphol., 48, 1–24.
- Zöller, L., D. Faust, and H. von Suchodoletz (2006), Pedostratigraphie des Quartärs auf Lanzarote, Bayreuther Geowiss. Arb., 27, 1–21.

**Tables**

*Table 1:* Properties of Studied Sites on Lanzarote

| | Femés | Guatiza | Teguise |
|---|---|---|---|
| Latitude N | 28°55′32′′ | 29°04′08′′ | 29°04′52′′ |
| longitude W | 13°45′19′′ | 13°29′22′′ | 13°30′55′′ |
| Altitude (m a.s.l.) | 300 | 100 | 300 |
| catchment area (km$^2$) | 5.07 | 10.1 | 3.8 |
| valley bottom (% of catchment area) | 18 | 16.1 | 35 |
| relative elevation difference in the catchment area (m) | 100 (SE slopes) – 200 (NW slopes) | > 550 | 100 |
| time of volcanic damming | 1.4 Ma[1] | 170 ka[2] | 1.2 Ma[3] |
| volcanic damming complete? | yes | no | no |
| thickness of anthropogenic colluvial deposits (cm) | 55 | 420 | 80 |

[1] Zöller et al. (2006)

[2] consistent thermoluminescence and ESR data (H. v. Suchodoletz et al., unpublished results, 2006)

[3] Instituto Tecnológico y Geominero de España [2008].

*Table 2 :* Kind and strengths of used irradiation-sources.

Strengths are given in Gy/min and referred to 21 August 2006, except for the external $^{90}$Sr/$^{90}$Y-source which is referred to 15 June 2006.

| type of irradiation | type of source | coarse grain | fine grain |
|---|---|---|---|
| B | $^{90}$Sr/$^{90}$Y (internal Risø-reader 1) | 8.81 | - |
| | $^{90}$Sr/$^{90}$Y (internal Risø-reader 2) | 2.57 | 2.52 |
| | $^{90}$Sr/$^{90}$Y (external) | - | 7.85 |
| A | Littlemore $^{241}$Am (external) | - | 1.26 |

***Table 3:*** Used measurement-parameters for OSL and IRSL

| | OSL | IRSL |
|---|---|---|
| Stimulation-LEDs | 470 ± 20 nm | 845 ± 20 nm |
| Detection-filter | U-340 Hoya (transmission 290 - 380 nm) | BG 39, GG 400, 2xBG 3 (transmission 390-450 nm) |
| Preheat (rate 10°/s) | 240°C for 10 s | 220°C for 120 s (age < 10 ka) 220°C for 300 s (age > 10 ka) |
| Cut-heat (rate 5°C/s) | 160°C | |
| Test dose | Reader 1: 2.2 Gy Reader 2: 0.64 Gy | |
| Measurement | 20 s at 125°C | 60 s at room temperature |
| Used integral | 0.0 - 0.4 s | 0 - 15 s |
| Background interval | 16 - 20 s | 55 - 60 s |

**Table 4:** Luminescence dating: Analytical results

Dose rates ($\dot{D}$) are given in Gy/ka. U- and Th-contents were calculated from the α –countrate. Measured water contents present the ratio moist/dry weight, the correction was done using the clay contents of the samples. The error of water contents is assumed to be 0.1.

| Sample depth (cm) | Sample | α - countrate (cpm) | U-content (ppm) | Th-content (ppm) | K-content (%) [1] from ICPMS [2] from AAS | $\dot{D}$ -β* | $\dot{D}$ -γ* | $\dot{D}$ cosm | Measured water content | Corrected water content |
|---|---|---|---|---|---|---|---|---|---|---|
| *Femés* | | | | | | | | | | |
| 60 | BT 310, (BN-D 207) | 0.58* | - | - | - | 2.58 ± 0.13 | 1.12 ± 0.06 | 0.21 ± 0.011 | 1.1* | 1.19 |
| 80 | BT 311 | 0.48 ± 0.012 | 2.34 ± 0.058 | 8.00 ± 0.20 | 2.45 ± 0.07[2] | - | - | 0.21 ± 0.010 | 1.13 | 1.24 |
| 100 | BT 189 | 0.46 ± 0.009 | 2.25 ± 0.044 | 7.70 ± 0.15 | 3.19 ± 0.10[1] | - | - | 0.20 ± 0.010 | 1.13 | 1.24 |
| 120 | BT 312 | 0.36 ± 0.008 | 1.75 ± 0.039 | 6.01 ± 0.13 | 3.32 ± 0.10[2] | - | - | 0.20 ± 0.010 | 1.13 | 1.24 |
| 140 | BT 313 | 0.43 ±0.006 | 2.09 ± 0.029 | 7.16 ± 0.10 | 2.12 ± 0.06[2] | - | - | 0.20 ± 0.010 | 1.14 | 1.22 |
| 170 | BT 190, (BN-D 209) | 0.47* | - | - | - | 3.25 ± 0.05 | 1.08 ± 0.05 | 0.19 ± 0.010 | 1.19* | 1.25 |
| 190 | BT 314 | 0.40 ± 0.008 | 1.96 ± 0.040 | 6.71 ± 0.14 | 1.91 ± 0.06[2] | - | - | 0.19 ± 0.010 | 1.17 | 1.26 |
| 210 | BT 315 | 0.44 ± 0.001 | 2.12 ± 0.004 | 7.25 ± 0.02 | 2.61 ± 0.08[2] | - | - | 0.19 ± 0.009 | 1.20 | 1.27 |
| 225 | BT 316 | 0.39 ± 0.010 | 1.87 ± 0.047 | 6.39 ± 0.16 | 2.66 ± 0.08[2] | - | - | 0.19 ± 0.009 | 1.20 | 1.28 |
| 245 | BT 317 | 0.41 ± | 2.01 ± 0.047 | 6.87 ± 0.16 | 2.99 ± 0.09[2] | - | - | 0.18 ± 0.009 | 1.19 | 1.30 |

| | | 0.010 | | | | | | | | |
|---|---|---|---|---|---|---|---|---|---|---|
| 270 | BT 224 | 0.44 ± 0.008 | 2.13 ± 0.039 | 7.28 ± 0.13 | 2.89 ± 0.09[1] | - | - | 0.18 ± 0.009 | 1.18 | 1.24 |
| 290 | BT 318 | 0.30 ± 0.008 | 1.46 ± 0.039 | 5.01 ±0.13 | 1.78 ± 0.05[2] | - | - | 0.18 ± 0.009 | 1.11 | 1.24 |
| 310 | BT 319 | 0.30 ± 0.006 | 1.46 ± 0.027 | 5.01 ± 0.09 | 2.07 ± 0.06[2] | - | - | 0.18 ± 0.009 | 1.11 | 1.23 |
| 330 | BT 301 | 0.44 ± 0.009 | 2.12 ± 0.044 | 7.27 ± 0.15 | 2.24 ± 0.07[2] | - | - | 0.17 ± 0.009 | 1.14 | 1.25 |
| 350 | BT 302 | 0.43 ± 0.010 | 2.09 ± 0.048 | 7.16 ± 0.17 | 1.70 ± 0.05[2] | - | - | 0.17 ± 0.009 | 1.18 | 1.28 |
| 380 (400*) | BN-D 211 | 0.45* | - | - | - | 3.27 ± 0.05 | 1.09 ± 0.06 | 0.17 ± 0.008 | 1.15* | 1.27 |
| 460 | BT 191 | 0.47 ± 0.010 | 2.28 ± 0.050 | 7.16 ± 0.17 | 3.39 ± 0.10[1] | - | - | 0.16 ± 0.008 | 1.12 | 1.26 |
| 480 | BT 303 | 0.44 ± 0.007 | 2.11 ± 0.034 | 7.23 ± 0.12 | 2.83 ± 0.08[1] | - | - | 0.15 ± 0.008 | 1.17 | 1.28 |
| 630 (670*) | BN-D 213 | 0.45* | - | - | - | 3.12 ± 0.16 | 0.99 ± 0.05 | 0.14 ± 0.007 | 1.30* | 1.3 |
| *Teguise* | | | | | | | | | | |
| 80 | BT 306 | 0.52 ± 0.018 | 2.5 ± 0.087 | 8.57 ± 0.30 | 2.53 ± 0.08[2] | - | - | 0.21 ± 0.010 | 1.05 | 1.16 |
| 90 | BT 198 | 0.65 ± 0.013 | 3.12 ± 0.061 | 10.70 ± 0.21 | 2.49 ± 0.07[1] | - | - | 0.21 ± 0.010 | 1.04 | 1.16 |
| 110 | BT 235 | 0.52 ± 0.010 | 2.51 ± 0.048 | 8.60 ± 0.17 | 2.86 ± 0.09[2] | - | - | 0.20 ± 0.010 | 1.09 | 1.27 |

| | | | | | | | | | | |
|---|---|---|---|---|---|---|---|---|---|---|
| 135 | BT 307 | 0.44 ± 0.016 | 2.11 ± 0.078 | 7.22 ± 0.27 | $3.19 \pm 0.10^{2}$ | - | - | 0.20 ± 0.010 | 1.19 | 1.28 |
| 160 | BT 199 | 0.46 ± 0.007 | 2.21 ± 0.033 | 7.57 ± 0.11 | $3.69 \pm 0.11^{1}$ | - | - | 0.20 ± 0.010 | 1.13 | 1.31 |
| 185 | BT 308 | 0.32 ± 0.006 | 1.56 ± 0.030 | 5.35 ± 0.10 | $2.24 \pm 0.07^{2}$ | - | - | 0.19 ± 0.010 | 1.14 | 1.26 |
| 210 | BT 309 | 0.39 ± 0.008 | 1.86 ± 0.039 | 6.38 ± 0.13 | $2.32 \pm 0.07^{2}$ | - | - | 0.19 ± 0.009 | 1.17 | 1.24 |
| 250 | BT 200 | 0.56 ± 0.010 | 2.69 ± 0.048 | 9.21 ± 0.17 | $2.90 \pm 0.09^{1}$ | - | - | 0.18 ± 0.009 | 1.1 | 1.26 |
| 330 | BT 236 | 0.40 ± 0.007 | 1.92 ± 0.034 | 6.57 ± 0.12 | $4.08 \pm 0.12^{1}$ | - | - | 0.17 ± 0.009 | 1.14 | 1.26 |
| 450 | BT 201 | 0.42 ± 0.009 | 2.05 ± 0.044 | 7.03 ± 0.15 | $3.73 \pm 0.11^{1}$ | - | - | 0.16 ± 0.008 | 1.18 | 1.26 |
| 610 | BT 202 | 0.43 ± 0.007 | 2.10 ± 0.034 | 7.19 ± 0.12 | $2.93 \pm 0.09^{1}$ | - | - | 0.14 ± 0.007 | 1.09 | 1.27 |
| *Guatiza III* | | | | | | | | | | |
| 110 | BT 193 | 0.39 ± 0.008 | 1.88 ± 0.039 | 6.44 ± 0.13 | $2.89 \pm 0.09^{1}$ | - | - | 0.2 ± 0.010 | 1.09 | 1.24 |
| 250 | BT 194 | 0.40 ± 0.009 | 1.96 ± 0.044 | 6.71 ± 0.15 | $2.53 \pm 0.08^{1}$ | - | - | 0.18 ± 0.009 | 1.10 | 1.26 |
| 435 | BT 195 | 0.51 ± 0.009 | 2.49 ± 0.044 | 8.53 ± 0.15 | $3.96 \pm 0.12^{1}$ | - | - | 0.16 ± 0.008 | 1.07 | 1.21 |
| 470 | BT 233 | 0.43 ± 0.006 | 2.06 ± 0.029 | 7.05 ± 0.10 | $2.51 \pm 0.08^{1}$ | - | - | 0.15 ± 0.008 | 1.11 | 1.25 |
| 495 | BT 196 | 0.48 ± | 2.35 ± 0.044 | 8.03 ± 0.15 | $2.73 \pm 0.08^{1}$ | - | - | 0.15 ± 0.008 | 1.08 | 1.25 |

| | | 0.009 | | | | | | | | |
|---|---|---|---|---|---|---|---|---|---|---|
| 550 | BT 234 | 0.44 ± 0.006 | 2.11 ± 0.029 | 7.22 ± 0.10 | 3.22 ± 0.10[1] | - | - | 0.15 ± 0.008 | 1.14 | 1.26 |
| 610 | BT 304 | 0.39 ± 0.011 | 1.90 ± 0.053 | 6.51 ± 0.18 | 4.02 ± 0.12[2] | - | - | 0.14 ± 0.007 | 1.13 | 1.28 |
| 660 | BT 197 | 0.53 ± 0.009 | 2.58 ± 0.044 | 8.84 ± 0.15 | 2.99 ± 0.09[1] | - | - | 0.14 ± 0.007 | 1.09 | 1.22 |
| 700 | BT 305 | 0.50 ± 0.013 | 2.43 ± 0.063 | 8.32 ± 0.22 | 3.86 ± 0.12[2] | - | - | 0.13 ± 0.007 | 1.11 | 1.23 |
| *Guatiza I* 210 | BN-D 219 | 0.46* | - | - | - | 2.58 ± 0.04 | 0.85 ± 0.04 | 0.18 ± 0.009 | 1.20 | - |
| *Tahiche* recent | BT 204 | 0.42 ± 0.009 | 2.04 ± 0.043 | 6.98 ± 0.15 | 2.00 ± 0.06[1] | - | - | 0.21 ± 0.011 | 1.10 | - |

* data taken from Zöller et al. [2003]

**Table 5:** Luminescence dating: Equivalent doses and ages

$D_e$´s are given in Gy. Coarse grain OSL-$D_e$´s were calculated after Juyal et al. [2006]. All ages are given in ka. Measured a-values are given in standard, assumed a-values in italic letters.

| Sample depth (cm) | Code | IRSL-$D_e$ | a-value IRSL | IRSL age | Anomalous Fading | Fine-grain quartz OSL-$D_e$ | a-value fine grain quartz OSL | Fine-grain quartz OSL age | Coarse-grain quartz OSL-$D_e$ | Coarse-grain quartz OSL age |
|---|---|---|---|---|---|---|---|---|---|---|
| *Femés* | | | | | | | | | | |
| 60 | BT 310 (BN-D 207) | 18.3 ± 4.7* | 0.04 ± 0.001* | 4.9 ± 1.3 | yes* | - | - | - | 20.5 ± 1.5 | 6.4 ± 0.7 |
| 80 | BT 311 | - | | - | - | - | - | - | 38.0 ± 3.4 | 12.4 ± 1.6 |
| 100 | BT 189 | 65.5 ± 0.8 | *0.04 ± 0.002* | 16.7 ± 1.5 | yes | 65.3 ± 4.9 | 0.03 ± 0.01 | 16.8 ± 1.9 | 47.9 ± 3.7 | 13.6 ± 1.6 |
| 120 | BT 312 | - | - | - | - | - | - | - | 122 ±11.9 | 35.4 ± 4.7 |
| 140 | BT 313 | - | - | - | - | - | - | - | 150 ± 10.8 | 56.0 ± 6.5 |
| 170 | BT 190 (BN-D 209) | 166 ± 12* | 0.04 ± 0.002* | 41.0 ± 3.8 | no* | - | - | - | 165 ± 31.4 | 45.9 ± 9.7 |
| 190 | BT 314 | - | - | - | - | - | - | - | 194 ± 22.6 | 55.9 ± 8.2 |
| 210 | BT 315 | - | - | - | - | - | - | - | 164 ± 22.8 | 47.7 ± 7.8 |
| 225 | BT 316 | - | - | - | - | - | - | - | 204 ± 25.1 | 54.8 ± 7.2 |
| 245 | BT 317 | - | - | - | - | - | - | - | 193 ± 17.4 | 57.6 ± 7.2 |
| 270 | BT 224 | 328 ± 2 | *0.04 ± 0.002* | 91.2 ± 8.1 | no | - | - | - | 208 ± 16.6 | 64.8 ± 7.8 |
| 290 | BT 318 | - | - | - | - | - | - | - | 213 ± 49.2 | 101.0 ± 24.9 |
| 310 | BT 319 | - | - | - | - | - | - | - | 219 ± 65.7 | 93.3 ± 29.2 |
| 330 | BT 301 | - | - | - | - | - | - | - | 237 ± 21.0 | 88.3 ± 11.1 |
| 350 | BT 302 | - | - | - | - | - | - | - | 275 ± 46.8 | 125.0 ± 23.8 |

| | | | | | | | | | | |
|---|---|---|---|---|---|---|---|---|---|---|
| 380 (400*) | BN-D 211 | 419 ± 46* | 0.04 ± 0.002* | 106 ± 15 | no* | - | - | - | - | - |
| 460 | BT 191 | 568 ± 3 | 0.04 ± 0.002 | 144 ± 13 | no | - | - | - | - | - |
| 480 | BT 303 | 529 ± 3 | 0.04 ± 0.002 | 156.3 ± 13.8 | no | - | - | - | - | - |
| 630 (670*) | BN-D 213 | 709 ± 79* | 0.03 ± 0.009* | 207 ± 27 | no* | - | - | - | - | - |
| *Teguise* | | | | | | | | | | |
| 80 | BT 306 | - | - | - | - | - | - | - | 18.1 ± 0.5 | 5.4 ± 0.6 |
| 90 | BT 198 | 36.2 ± 0.4 | 0.06 ± 0.001 | 8.3 ± 0.8 | no | 35.3 ± 1.5 | 0.05 ± 0.013 | 8.5 ± 0.9 | 25.7 ± 0.9 | 7.2 ± 0.8 |
| 110 | BT 235 | - | - | - | - | - | - | - | 72.1 ± 4.3 | 22.0 ± 2.3 |
| 135 | BT 307 | - | - | - | - | - | - | - | 103 ± 6.1 | 30.7 ± 3.2 |
| 160 | BT 199 | 287 ± 3 | 0.06 ± 0.0004 | 68 ± 6.2 | yes | - | - | - | 163 ± 11.5 | 44.4 ± 4.9 |
| 185 | BT 308 | - | - | - | - | - | - | - | 172 ± 15.9 | 69.4 ± 6.0 |
| 210 | BT 309 | - | - | - | - | - | - | - | 327 ± 47.8 | 121.6 ± 10.8 |
| 250 | BT 200 | 485 ± 1.4 | 0.06 ± 0.0003 | 121.3 ± 11 | yes | - | - | - | 386 ± 67 | 114.3 ± 22.3 |
| 330 | BT 236 | 583 ± 2 | 0.06 ± 0.0005 | 129.3 ± 11.5 | no | - | - | - | - | - |
| 450 | BT 201 | 592 ± 2 | 0.06 ± 0.0005 | 138.0 ± 12.3 | yes | - | - | - | - | - |
| 610 | BT 202 | 688 ± 3 | 0.06 ± 0.0005 | 189.1 ± 16.7 | no | - | - | - | - | - |

| Guatiza III | | | | | | | | | | |
|---|---|---|---|---|---|---|---|---|---|---|
| 110 | BT 193 | 8.7 ± 0.2 | 0.05 ± 0.001 | 2.4 ± 0.2 | no | 8.2 ± 0.8 | *0.04 ± 0.007* | 2.3 ± 0.3 | 1.77 ± 0.2 | 0.54 ± 0.07 |
| 250 | BT 194 | - | - | - | - | 5.6 ± 0.2 | *0.04 ± 0.007* | 1.8 ± 0.2 | - | - |
| 435 | BT 195 | 16.5 ± 0.5 | 0.06 ± 0.003 | 3.4 ± 0.3 | no | - | - | - | 11.6 ± 0.5 | 2.7 ± 0.3 |
| 470 | BT 233 | 42.0 ± 0.4 | 0.04 ± 0.0004 | 13.0 ± 1.1 | no | 43.9 ± 2 | 0.04 ± 0.005 | 13.6 ± 1.3 | 36.7 ± 2.9 | 12.9 ± 1.5 |
| 495 | BT 196 | 113 ± 2 | 0.03 ± 0.001 | 32.4 ± 2.9 | no | 109 ± 2 | 0.04 ± 0.002 | 30.1 ± 2.7 | 99.4 ± 14.1 | 31.9 ± 5.4 |
| 550 | BT 234 | 99.7 ± 0.8 | *0.05 ± 0.001* | 26.1 ± 2.3 | yes | - | - | - | 168 ± 9.1 | 49.7 ± 5.2 |
| 610 | BT 304 | 138 ± 0.7 | *0.05 ± 0.001* | 32.3 ± 2.9 | no | 174 ± 9.5 | 0.04 ± 0.004 | 41.0 ±4.3 | - | - |
| 660 | BT 197 | 153 ± 2.5 | 0.05 ± 0.001 | 37.7 ± 3.4 | yes | - | - | - | 115 ± 19.9 | 33.0 ± 6.5 |
| 700 | BT 305 | 258 ± 2.4 | *0.05 ± 0.001* | 55.9 ± 5.0 | no | 211 ± 25 | 0.04 ± 0.007 | 46.2 ± 6.6 | - | - |
| Guatiza I | | | | | | | | | | |
| 210 | BT | 15.7 ± 1.3* | 0.08 ± 0.025* | 4.3 ± 0.5 | yes | - | - | - | 3.5 ± 0.2 | 1.2 ± 0.1 |
| Tahiche recent | BT 204 | 7.3 ± 0.3 | 0.05 ± 0.001 | 2.2 ± 0.2 | no | 6.3 ± 0.6 | *0.04 ± 0.007* | 2.1 ± 0.3 | 3.5 ± 1 | 1.2 ± 0.4 |

* data taken from Zöller et al. [2003]

# Figures

*Figure 1.* Location map of the island of Lanzarote with the studied vegas of Femés, Teguise, and Guatiza III. In addition, marine sediment cores from nearby locations are indicated in the inset.
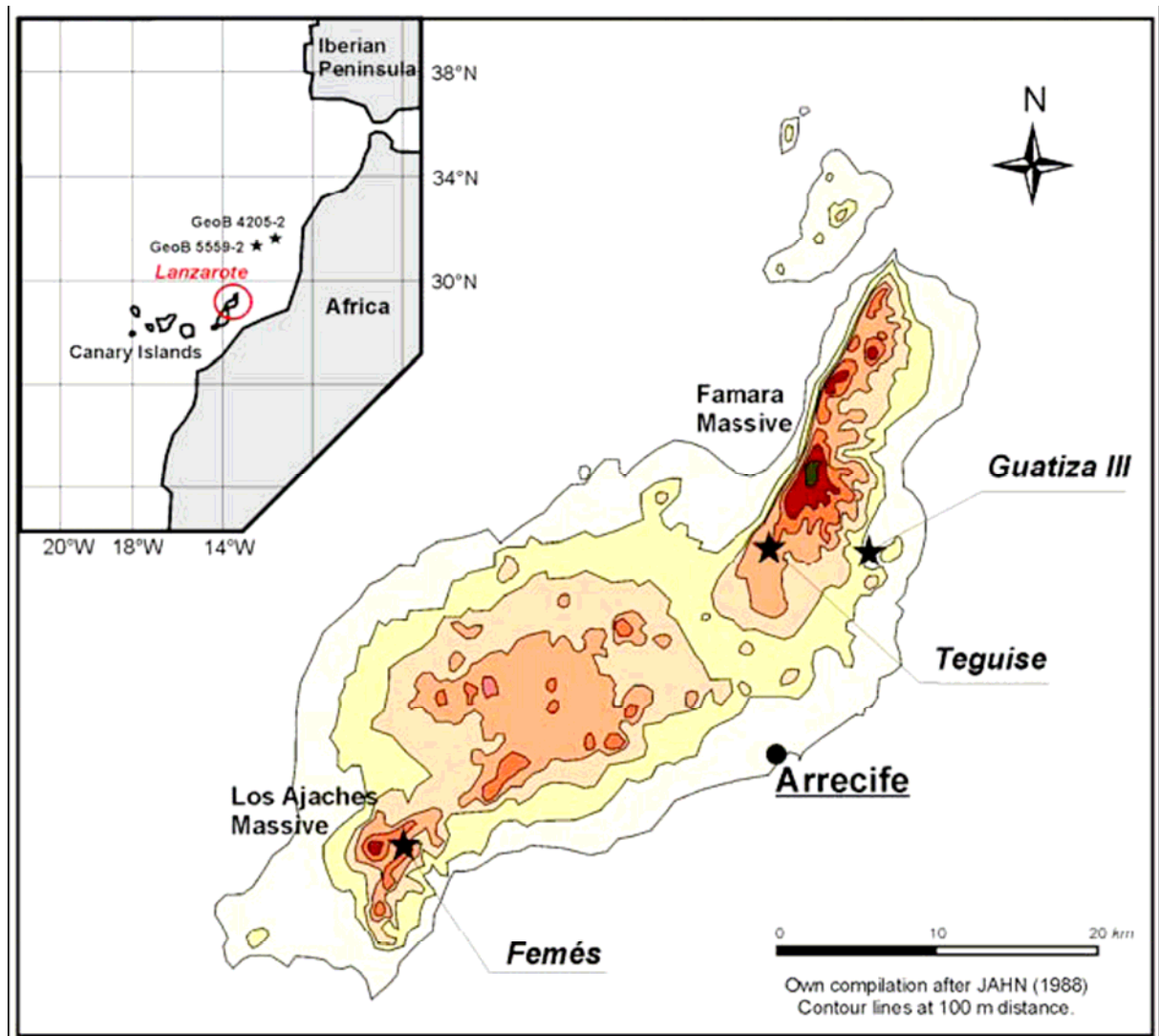
**Figure 2.** Profiles of (a) Femés, (b) Guatiza, and (c) Teguise. Given is the sedimentary character of the profiles and indicated are the sample locations for luminescence dating with their lab numbers.
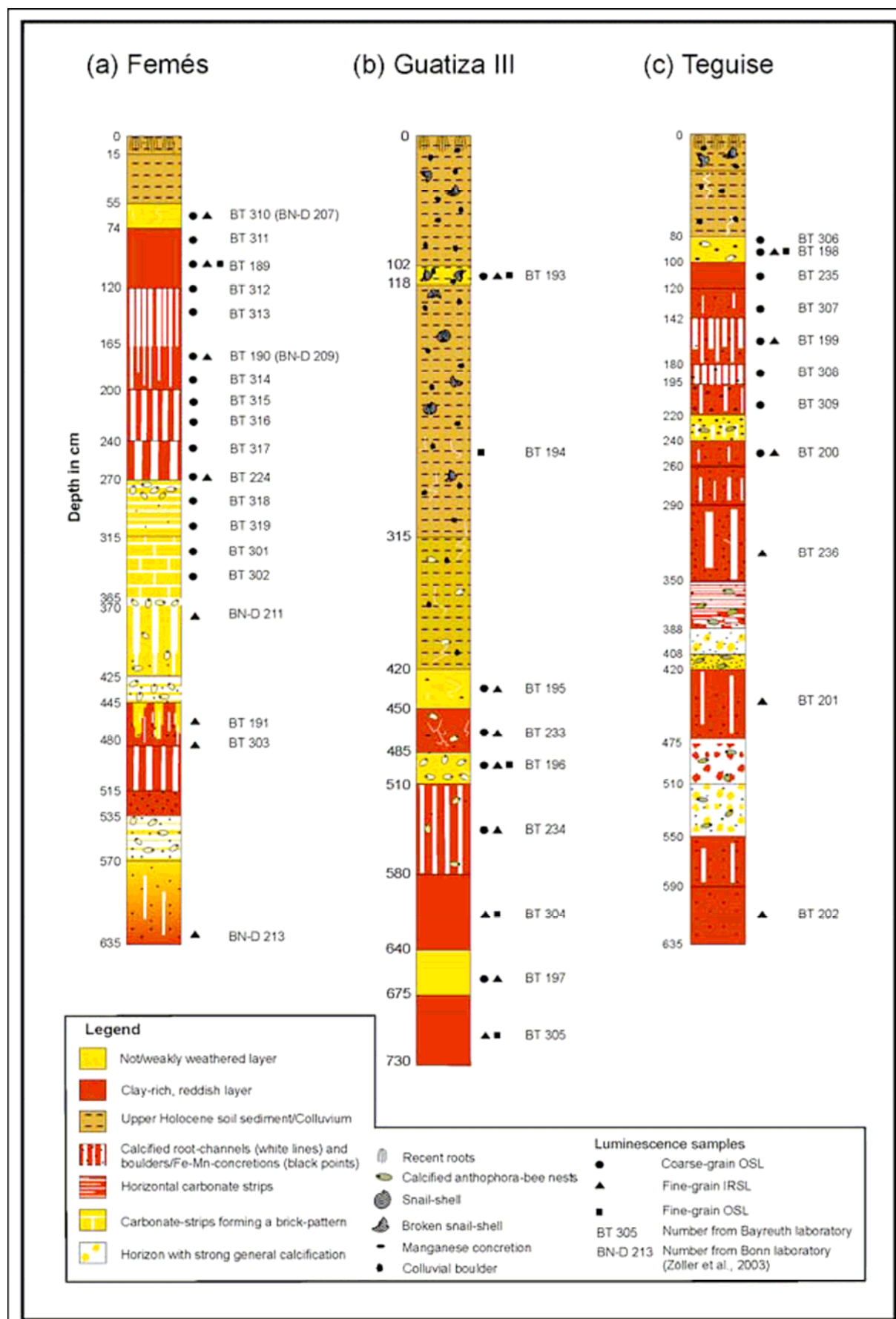
**Figure 3.** Selected De histograms of rather poorly bleached coarse-grain OSL samples from Teguise. Note the younger outlier in sample BT 308. In black are indicated calculated De after Juyal et al. [2006] and arithmetic means: u, uncorrected values; c, corrected values after removal of the upper 5% quantil; m, arithmetic mean.
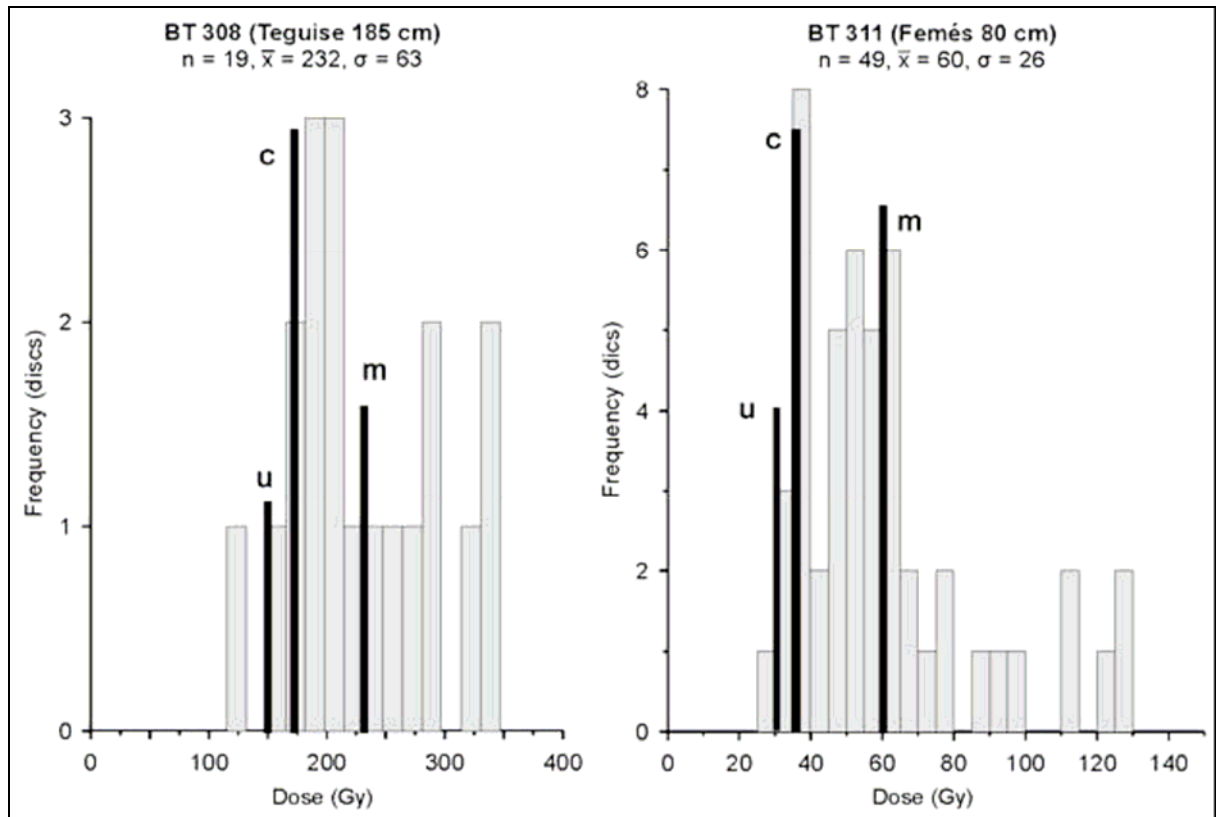
**Figure 4.** Results of the dose recovery test of coarsegrain samples measured with OSL, shown with error bars (2σ). Every data point is the average of four single measurements. Dashed lines below a graph indicate the given paleodose. Mean ratios given/measured dose were: 220°C, 1.08; 440°C, 1.09; 260°C, 1.1; 280°C, 1.07.
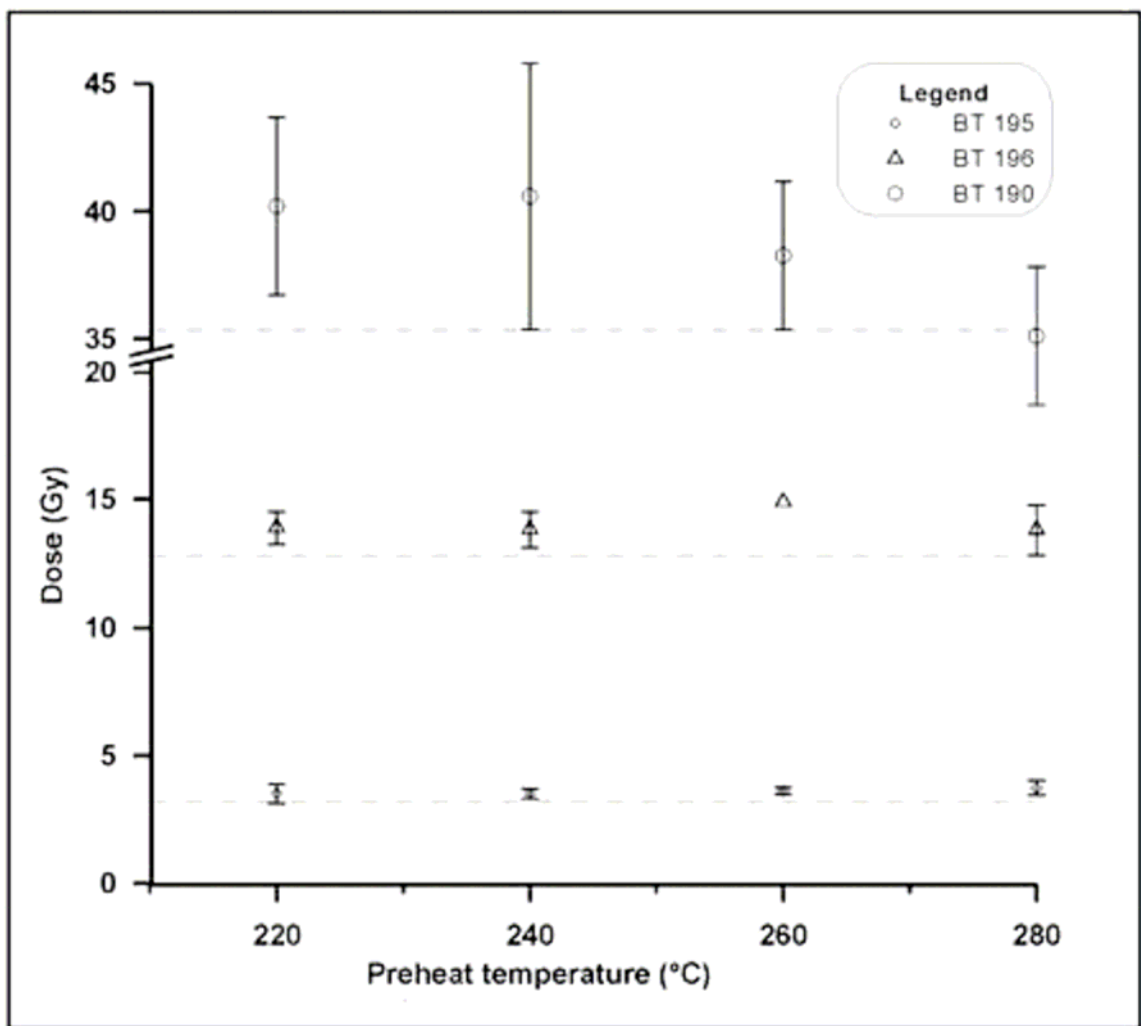
**Figure 5.** De histograms of coarse-grain OSL samples (a) BT 200 and (b) BT 197 with different De.
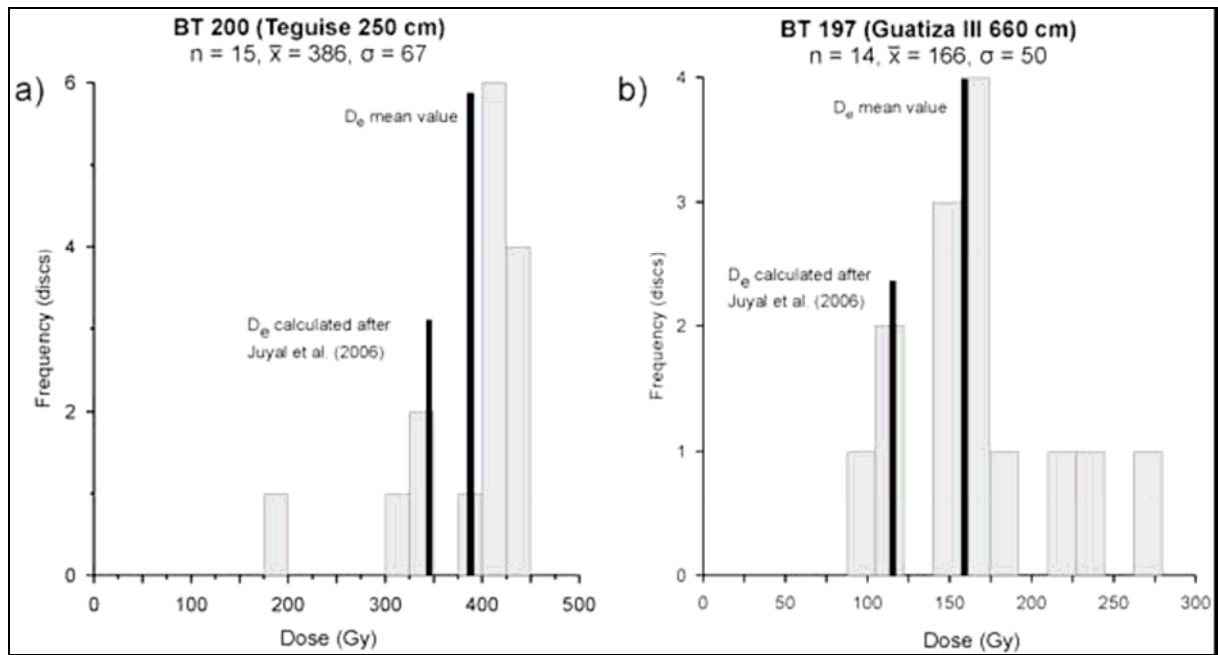
**Figure 6.** Vega stratigraphies with relative kaolinite contents adjusted to numerical chronostratigraphy and to marine Al and Fe contents. Luminescence dates giving correct sedimentation ages are shown with their error bars (in kiloannums), whereas the minimum age of sample BT 197 not presented. Shadowed areas in the profiles indicate generally unweathered/less weathered layers visible in the field and used for correlation between the vegas. Horizon depths in centimeters (not in scale) are indicated on the left side of the profiles.
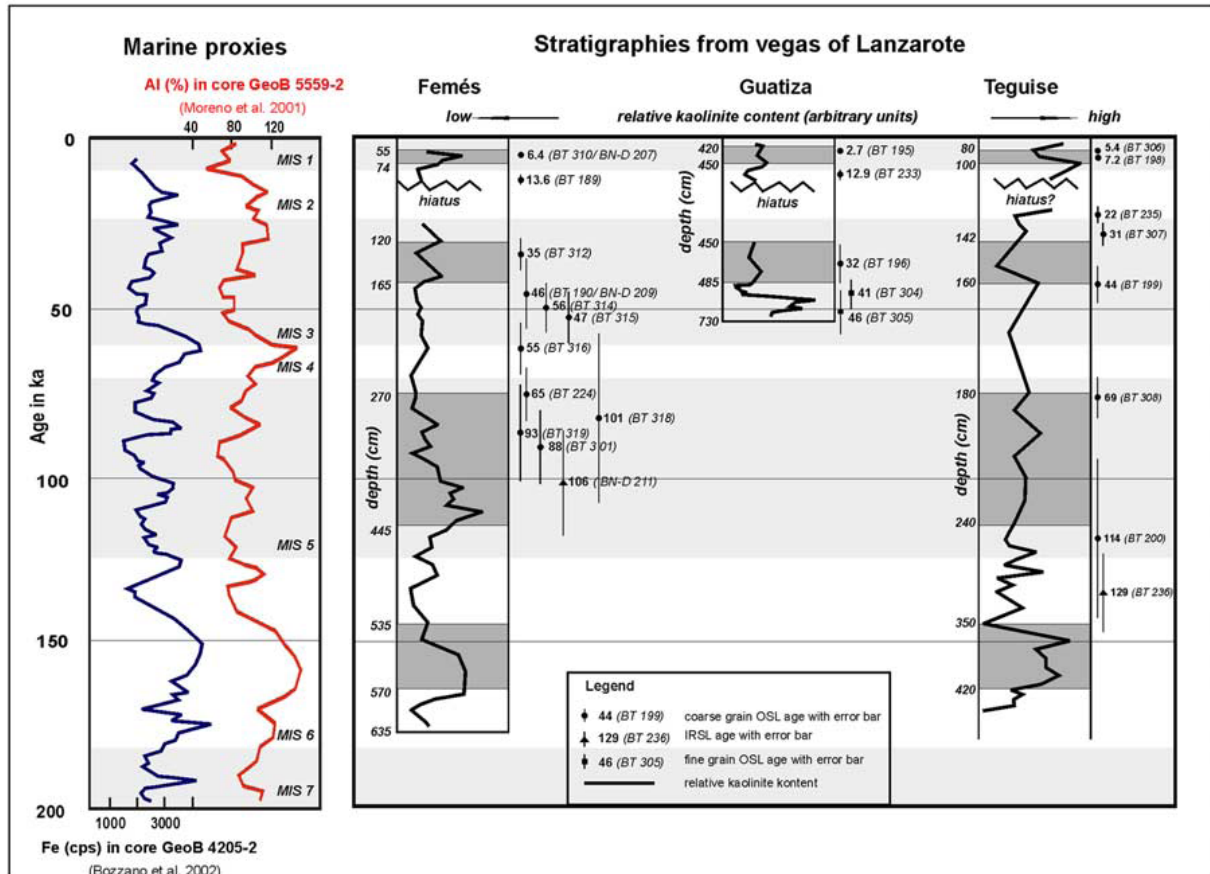
***Figure 7.*** Overview of measured luminescence ages with hiatae. Reliable and unreliable ages are discriminated.